Reachable Sets for Dubins Car in Control Problems: Physical Visualization

Starodubtsev I.S.
IMM UB RAS[1]
Russia, Ekaterinburg
starodubtsevis@imm.uran.ru

Fedotov A.A.
IMM UB RAS[1]
Russia, Ekaterinburg
andreyfedotov@mail.ru

Averbukh V.L.
IMM UB RAS[1]
Russia, Ekaterinburg
averbukh@imm.uran.ru

Patsko V.S.
IMM UB RAS[1]
Russia, Ekaterinburg
patsko@imm.uran.ru

ABSTRACT

The work deals with an application of the 3D-printing to full-size building the reachable sets in control problems. As an example, a simple car model is considered with nonlinear dynamics, three-dimensional phase vector, and scalar control constrained by modulus (Dubins car). Current state of the sytem includes its position in the plane and the velocity heading. The velocity value is given to be constant. The reachable sets are considered "at the terminal instant" and "till the terminal instant". These sets are nonconvex and their boundaries are not smooth in the whole. Peculiarities of the sets can be better comprehended being represented in the form of three-dimensional bodies that are built with using the 3D-printing. The sets' boundaries are presented in the VRML and STL formats. Examples of computation and visualization are given including their 3D-printed copies. Problems are discussed that appear under the 3D-constructing of surfaces with complicated forms.

Keywords
control problems, reachable sets, 3D-printing, FDM-printing, physical visualization

1 INTRODUCTION

Let a control system dynamics be described by a stationary vector differential equation $\dot{z} = f(z, u)$ with a geometric constraint $u(t) \in P$, and $z(t; z_0, u(\cdot))$ be a system position at the instant t on a trajectory beginning from the initial point z_0 at the instant $t_0 = 0$. Then *the reachable set at a fixed instant T* is

$$G(T; z_0) = \bigcup_{u(\cdot)} z(T; z_0, u(\cdot)).$$

The join is performed over all *admissible controls $u(\cdot)$*. In many cases, the reachable set is closed in the class of piecewise-continuous controls. So, as admissible controls $u(\cdot)$, we can take piecewise-continuous functions $t \to u(t)$.

The reachable set $G(T; z_0)$ at the fixed instant T comprises of all points, to which the control system can be delivered (by means of admissible controls) at the given instant T from the initial point z_0 given at the instant $t_0 = 0$. If for a stationary system we say about the reachable set $G^*(T; z_0)$ *till the instant T*, then

[1] Krasovskii Institute of Mathematics and Mechanics, Ekaterinburg, Russia

$$G^*(T; z_0) = \bigcup_{t \in [0, T]} \bigcup_{u(\cdot)} z(t; z_0, u(\cdot)).$$

Here, the join is additionally performed over all instants $t \in [0, T]$.

Appearance of 3D-printers opens opportunity of full-scale visualization of three-dimensional reachable sets. Such three-dimensional bodies performed on the 3D-printer make easy comprehension of geometry of the reachable sets.

An adequate physical visualization gets off the "mysticism" and connected with it "fear" of students and engineers to use results of the mathematical control theory to investigate and solve applied problems.

At the same time, apparency of comprehension can suggest such "reasonable" variants of approximation for three-dimensional objects, for which the most important quality characteristics of the objects are not lost.

2 CONTROL PROBLEM

Let the reachable sets be investigated *at the instant* and *till the instant* for a simple model of car motion (Dubins car [5, 6]). The dynamics is described as follows:

$$\begin{aligned}
\dot{x} &= V \cos \varphi, \\
\dot{y} &= V \sin \varphi, \\
\dot{\varphi} &= \frac{k}{V} u, \\
|u| &\leq 1, \ V = \text{const} > 0, \ k = \text{const} > 0,
\end{aligned} \tag{1}$$

where x, y are coordinates of the geometric position, φ is the heading of the velocity vector (Fig. 1), V is

the velocity value, k is the maximal value of the lateral acceleration. Admissible controls $u(\cdot)$ are piecewise-continuous functions of time that satisfy the constraint $|u(t)| \leq 1$. Values of the heading angle φ are considered in the interval $(-\infty, +\infty)$.
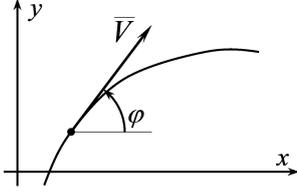

Figure 1: System of coordinates.

The system phase vector (x, y, φ) (1) is denoted as z. To be short, assume $\alpha = k/V$. Peculiarity of system (1) is in the fact that the initial state z_0 affects onto the reachable set with accuracy up to a turn and transfer. So, assume $z_0 = 0$ and write $G(T)$, $G^*(T)$ instead of $G(T; z_0)$, $G^*(T; z_0)$.

In paper [2], the form of the reachable sets $G(T)$ was found in projection onto the plane of geometric coordinates x, y. In [7], the reachable sets $G(T)$ were investigated in the three-dimensional space x, y, φ.

In work [3], the reachable sets $G^*(T)$ were investigated. Also, the sets $G(T)$ and $G^*(T)$ were considered under nonsymmetric constraints onto the control u.

3 PREPARATION OF DATA FOR A 3D-PRINTER

To obtain for system (1) computer images of the reachable sets, the VRML (v2.0) format was used.

It was proved in [7], that the boundary of the reachable set $G(T)$ under the symmetric constraint $|u| \leq 1$ comprises of six surfaces given in the three-dimensional space and defined by two parameters. These parameters are the instants of the control switches.

One of these surfaces corresponds to the control values $-1, 0, 1$ that are performed in time namely in the shown order. In this case, the parameter t_1 corresponds to the instant of the control switching from the value -1 to 0, and the parameter $t_2 \in [t_1, T]$ corresponds to the control switching from the value 0 to 1.

Other five surfaces correspond to the control collections $1, 0, -1$; $1, 0, 1$; $-1, 0, -1$; $1, -1, 1$; $-1, 1, -1$.

For each of the surfaces mentioned above, a uniform time-step grid is given for forming collection of the switch instants. Instants 0 and T are formally included into this collection. Note that the third equation of system (3) is stationary and linear w.r.t. the control u. So, values $\varphi(T)$ at an instant T also belong to nodes of the uniform grid on φ. Under this, an interval of possible values of φ is $[0, \alpha T]$ for the control version +1, 0, +1; $[-\alpha T, 0]$ for control -1, 0, -1; and $[-\alpha T, \alpha T]$ for all other four versions of control. This allows one

to provide layer-after-layer constructing the considered surfaces with a uniform step in φ.

It is important to note that for correct junction of neighboring surfaces, it becomes possible to choose special time steps of different surfaces in such a way that the set in φ will be the same for all set $G(T)$. To do this in practical constructing of the surfaces, the interval $\pm \alpha T$ of admissible values of φ is divided into even number $2m$ of equal segments to include the zero value. For each node in the interval of φ, possible motions of system (1) are calculated on the interval $[0, T]$ from the point z_0 by application of a concrete version of the control changes.

Under this, the step of over-looking the switching instants for surfaces determined by control collections ± 1, 0, ± 1, and ± 1, 0, ∓ 1 coincides with the step of dividing the interval on φ and is equal to $\alpha T / m$. For two other surfaces, the step of over-looking the switching instants is given twice smaller.

It should be noted some peculiarites of surfaces (composing boundary of the reachable set $G(T)$). As a rule the quantity of points from a layer to layer in φ differs not more than on 1. For the outer layer, consisting of a single point, the difference in number of points with the neighboring layer may be more then 1. This is used for correct junction of layers by means of collections of spatial triangle elements (i.e., by triangulation) during process of forming corresponding three-dimensional objects in formats VRML and STL.

In the case of nonsymmetric constraint on the control u, the difference is in the fact that the general interval of admissible values of φ is not symmetric w.r.t. zero.

In preparation for 3D-printing the sets $G^*(T)$, the data are firstly formed for building the sets $G(T)$. After that to them, the collections of the space-triangle elements are added. Note that these collections have been built during procession of the layers obtained on the grid of instants from 0 till T under marginal controls with only one switch instant as a parameter [3].

Thus, in all cases, a collection of surfaces (containing boundary of the reachable set) is written into a text-file in the STL format. The surfaces' parts that are not on the boundary of the reachable set are placed inside the object to be formed. Triangulation of the surfaces is performed "layer-after-layer" with using the property of continuity of cross-sections on φ for the reachable sets at the instant and on t for the additional surface for the reachable sets till the instant.

4 3D-PRINTING THE REACHABLE SETS

Several versions of reachable sets *at the instant* and *till the instant* have been prepared and printed on the 3D-printer (RepRap Prusa i3 style).

Fig. 2 presents the set $G^*(T)$ till the instant $T = 1.5\pi/\alpha$ (left) and the set $G(T)$ at the instant $T = 1.5\pi/\alpha$ (right). Fig. 3 shows the reachable sets $G(T)$ at the instants $T = 2\pi/\alpha$, $3\pi/\alpha$, $4\pi/\alpha$. Nonsimmetric reachable set $G(T)$ for $T = 5\pi/\alpha$ and $u \in [-1, +0.25]$ is shown in Fig. 4.
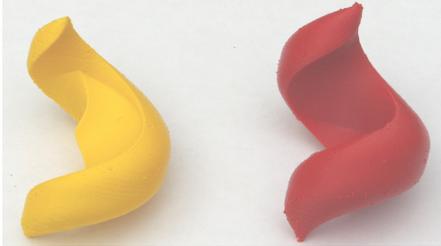
Figure 2: The reachable sets $G^*(T)$ and $G(T)$ for $T = 1.5\pi/\alpha$.
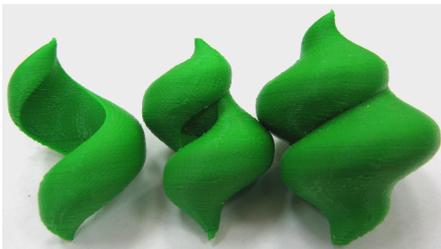
Figure 3: The sets $G(T)$ at $T = 2\pi/\alpha$, $3\pi/\alpha$, $4\pi/\alpha$.

Figure 4: The reachable sets $G(T)$ at $T = 5\pi/\alpha$ in the case $u \in [-1, +0.25]$.

Last years, investigations in physical visualization and, particular, in the 3D-printing, become more and more popular. In work [4], a review is given of application of such technologies in various branches of science and medicine.

Methods of 3D-printing claim more strict demands to a visualized object in comparison with visualization by usual traditional means of computer graphics.

Introduce the following notions:

• *Slicer* is a program for transferring a 3D-model into a controlling code for the printer; this program is necessary since the printer will not be able to load directly the 3D-model; also, there are printers, in which the slicer already is a part of the internal software;

• *Slicing* is a process of transferring the 3D-model into the controlling code.

There exist several types of the 3D-printing that use different technologies and materials. For visualization of the reachable sets, we have used the FDM (Fused Deposition Modeling) printing technology by molten thread (fiber) of the ABS plastic.

The model is cut (sliced) into layers. Each layer are includes the perimeters, infilling, and/or supports. A model can have different level of the infilling, and it can also be without the infilling (a hollow model).

4.1 Peculiarities of the FDM-technology of printing

Below, we describe several facts that might not be classified as "problems". Rather, they can be regarded as peculiarities of the used technology that also should be taking into account for obtaining correct results.

1. Wall's thickness. The walls should be equal to the sprayer's diameter or thicker it. Otherwise, the printer will not be able to correct print them. The wall thickness depends on the sprayer's diameter and number of perimeters to be printed. For example, under three perimeters and sprayer's diameter 0.4 mm, the wall thickness must be 0.4, 0.8, 1.2, 1.6, and 2 mm, but got the larger number the thickness can be any one. So, the wall thickness should be multiple to the sprayer's diameter if it is smaller than $N \cdot d$, where N is the number of perimeters d is the sprayer's diameter.

2. Orientation of the object. The final result of printing can depend on the object orientation. Note the following aspects:

• Since the discrete character of slicing, the horizontal over-layering is imaged on the printed surface; this is the essence of 3D-printing by the FDM technology; to minimize the over-layering, it is possible to change the spatial orientation of the model or to use it to underline the model edges;

• Cylindric edges printed from the side surface can be "lower round" than the similar edges printed in the vertical projection;

• Stiffness/length: thin and direct elements will be more steady if they have been printed rather in the horizontal position than in the vertical one; this is stipulated by the fact that connections between layers are lower strong than inside one layer.

3. Overhanging elements. For each overhanging element (examples are given in Fig. 5), a supporting construction (the support) is necessary; the smaller number of overhanging elements, the smaller number of supports is necessary; so, expenditure of the plastic material and time of printing decrease; moreover, the support deforms the surface touching it.

4. Accuracy. Printing accuracy on axes XY depends on slacks, stiffness of construction, belts, and other details of the printer; for unprofessional printers, the accuracy is about 0.3 mm; accuracy along the axis Z is defined by
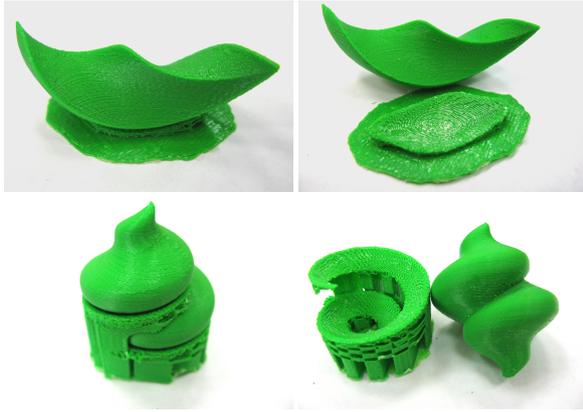
Figure 5: Examples of stable supports during printing for the reachable sets till the instant $T = \pi/\alpha$ (the upper row) and till the instant $T = 4\pi/\alpha$ (the lower row).

the layer height (0.1– 0.4 mm); so, hight of the model will be multiple to the layer height.

There exists and a software problem: not each slicer correctly processes the internal sizes; so, it would be better to increase the holes' diameters on 0.1 – 0.2 mm.

5. Changing the geometry. It is necessary to take into account that after cooling, the material shrinks out; so, the geometry of the printed object changes. On large objects, this can lead to "downturn" of the object's ends and, in some cases, to "detachment" of the printing model from the print table.

Another aspect of the thermo-shrinkage is in appearance of internal stress in the material. If the complete filling of the model was made, then under sufficient square of a cross-section, forces of the internal stress could lead to deforming (up to a break) the printed model. So, a partial filling of model is used in the form of various configurations of the uniform grid. As a result, the following features are provided:

• Compensation of the internal stresses;

• Increasing the model stiffness; the partial filling forms the stiffening ribs that do not allow deforming for the noncooled soft parts of the model under their own weight;

• Decrease of the material expenditure and time of printing.

In printing the reachable sets, we often used configuration of the internal filling in the form of a *square net*. In this case, the minimal value of material is necessary and the printing time is the shortest.

Some of the mentioned peculiarities are taken into account automatically (by the slicer or by the printer software). For example, a formation of the structure of internal filling or calculation of the support elements implemented automatically; but a user check such parameters as "density", "frequency" of the step, and the bevel angle under which it is necessary to built the support.

Other peculiarities have to be processed by-hand, since in the case of ambiguity (a hole in geometry, nonuniformity of the grid, improper normals) the result of procession could be unpredictable.

5 CONCLUSION

The paper describes results of practical calculations of the reachable sets and their reproduction (visualization) by means of 3D-printing for a dynamic object known as "Dubins car".

The sets have nontrivial geometry. Nevertheless, as a result of processing the obtained spatial objects, it was succeeded to achieve not only good quality of the three-dimensional printed images, but, also, to formulate criteria necessary for successful physical visualization.

When preparing this paper, the authors became aware that a close 3D-printing work was done [1] at Mines Paristech / LAAS-CNRS by G. Caner under the supervision by J.-P. Laumond. Namely, reachable sets till the instant were built for the Dubins car, as well as for the Reeds-Shepp car, by means of a 3D-printer. A mathematical model of the Reeds-Shepp car is also widely used in robotics and is described in [5, 6].

6 ACKNOWLEDGMENTS

7 REFERENCES

[1] Caner G. Modelisation en 3D de la boule de Reeds & Shepp. Rapport de stage d'option, Mines Paristech, LAAS-CNRS, 2015.

[2] Cockayne E. J., Hall G. W. C. Plane motion of a particle subject to curvature constraints. SIAM J. Control. Vol. 13, No. 1, pp. 197–220, 1975.

[3] Fedotov A. A., Patsko V. S., Turova V. L. Reachable sets for simple models of car motion. Ed. by A. V. Topalov. Rijeka: InTech Open Access Publisher, pp. 147–172, 2011.

[4] Horvath J. Mastering 3D Printing (1st edition). Berkely, CA, USA: Apress, 2014.

[5] Laumond J.-P. (ed.) Robot Motion Planning and Control. Lect. Notes in Contr. and Inform. Sci. Vol. 229. Springer, New York, 1998.

[6] Laumond J.-P., Mansard N., Lasserre J.-B. Optimality in robot motion: Optimal versus optimized motion. Communications of the ACM. Vol. 57, No. 9, pp. 82–89, 2014.

[7] Patsko V. S., Pyatko S. G., Fedotov A. A. Three-dimensional reachability set for a nonlinear control system. Journal of Computer and Systems Sciences International. Vol. 42, No. 3, pp. 320–328, 2003.